Fractal Powers in Serrin's Swirling Vortex Solutions

Pavel Bělík
Doug Dokken
Kurt Scholz
Misha Shvartsman

Mathematics Departments
Augsburg College
University of St. Thomas

JMM
San Diego, CA
January 10, 2013

Outline

1. Motivation and Axisymmetric Flow
2. Serrin's Swirling Vortex
3. Viscous Case ($\nu > 0$)
4. Inviscid Case ($\nu = 0$)
5. Conclusions

Outline

Motivation and Axisymmetric Flow

Motivation and Axisymmetric Flow

Serrin [1972]. The swirling vortex. Phil. Trans. Roy. Soc. London, Series A, Math & Phys. Sci., **271**, 325–360

Motivation and Axisymmetric Flow

Serrin [1972]. The swirling vortex. Phil. Trans. Roy. Soc. London, Series A, Math & Phys. Sci., **271**, 325–360

$$\text{velocity} \sim \frac{1}{r}$$

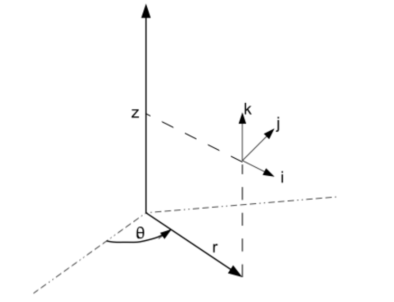

Motivation and Axisymmetric Flow

Cai [2005], Comparison between tornadic and nontornadic mesocyclones using the vorticity (pseudovorticity) line technique,
Mon. Wea. Rev., **133**, 2535–2551.

Wurman and Alexander [2005], The 30 May 1998 Spencer, South Dakota, Storm. Part II, Mon. Wea. Rev., **133**, 97–119.

Wurman and Gill [2000], Finescale Radar Observations of the Dimmitt, Texas (2 June 1995), Tornado, Mon. Wea. Rev., **128**, 2135–2164.

Motivation and Axisymmetric Flow

Cai [2005], Comparison between tornadic and nontornadic mesocyclones using the vorticity (pseudovorticity) line technique,
Mon. Wea. Rev., **133**, 2535–2551.

Wurman and Alexander [2005], The 30 May 1998 Spencer, South Dakota, Storm. Part II, Mon. Wea. Rev., **133**, 97–119.

Wurman and Gill [2000], Finescale Radar Observations of the Dimmitt, Texas (2 June 1995), Tornado, Mon. Wea. Rev., **128**, 2135–2164.

$$\text{velocity} \sim \frac{1}{r^b}, \quad b \text{ is in some range of values}$$

Governing Equations and Velocity Components

Navier–Stokes and Continuity Equations:

$$(\mathbf{v} \cdot \nabla)\mathbf{v} = -\nabla p + \nu\, \Delta \mathbf{v}$$

$$\nabla \cdot \mathbf{v} = 0$$

Governing Equations and Velocity Components

Navier–Stokes and Continuity Equations:

$$(\mathbf{v} \cdot \nabla)\mathbf{v} = -\nabla p + \nu \, \Delta \mathbf{v}$$

$$\nabla \cdot \mathbf{v} = 0$$

Assumptions on Velocity:

Spherical coordinates: (R, α, θ),

$$v_R = \frac{G(x)}{r^b}, \qquad v_\alpha = \frac{F(x)}{r^b}, \qquad v_\theta = \frac{\Omega(x)}{r^b},$$

$$x = \cos\alpha, \; r = R\sin\alpha, \; b > 0$$

Reduced Form of Navier–Stokes Equations

$$C_3(\alpha) = \nu R^{b-1} D_3(\alpha),$$
$$\dot{C}_1(\alpha) + 2b\, C_2(\alpha) = \nu R^{b-1} \frac{2b}{1+b} \left(\dot{D}_1(\alpha) + (1+b) D_2(\alpha) \right),$$

and

$$p(R,\alpha) = \frac{C_1(\alpha)}{2b\, R^{2b}} - \nu \frac{D_1(\alpha)}{(1+b) R^{1+b}} + \text{const.},$$

C_i and D_i are functions of F, G, Ω.

Continuity imposes some additional requirements on F, G, Ω.

Outline

Reduced Form of Navier–Stokes Equations ($b = 1$)

$$\nu(1-x^2)F^{(4)}(x) - 4\nu x F'''(x) + F(x)F'''(x) + 3F'(x)F''(x) = -\frac{2\Omega(x)\Omega'(x)}{1-x^2}$$

$$\nu(1-x^2)\Omega''(x) + F(x)\Omega'(x) = 0$$

Reduced Form of Navier–Stokes Equations ($b = 1$)

$$\nu(1-x^2)F^{(4)}(x) - 4\nu x F'''(x) + F(x)F'''(x) + 3F'(x)F''(x) = -\frac{2\Omega(x)\Omega'(x)}{1-x^2}$$

$$\nu(1-x^2)\Omega''(x) + F(x)\Omega'(x) = 0$$

Three types of solutions:

- Downdraft core with radial outflow (A)
- Downdraft core with a compensating radial inflow (B)
- Updraft core with radial inflow (C)

Reduced Form of Navier–Stokes Equations ($b = 1$)

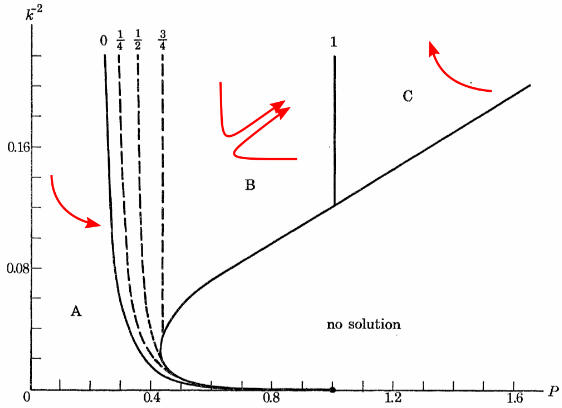

FIGURE 1. (P, k^{-2}) parameter diagram.

Outline

AUGSBURG COLLEGE UNIVERSITY of ST. THOMAS

Viscous Case: $b \neq 1$

$\nu > 0$, $b \neq 1$, the system of ODE's:

$$C_3(x) = 0, \qquad D_3(x) = 0,$$
$$\dot{C}_1(x) + 2b\, C_2(x) = 0, \qquad \dot{D}_1(x) + (1+b)D_2(x) = 0.$$

Viscous Case: $b \neq 1$

$\nu > 0$, $b \neq 1$, the system of ODE's:

$$C_3(x) = 0, \qquad D_3(x) = 0,$$
$$\dot{C}_1(x) + 2b\, C_2(x) = 0, \qquad \dot{D}_1(x) + (1+b) D_2(x) = 0.$$

Nonexistence of Solutions

When $\nu > 0$ and $b \neq 1$, no solutions of the form $\mathbf{v} = \dfrac{\mathbf{K}(x)}{r^b}$ exist.

AUGSBURG COLLEGE | UNIVERSITY of ST. THOMAS

Outline

Inviscid Case: "Negative" Results

The Euler equations: $C_3(x) = 0, \quad \dot{C}_1(x) + 2b\, C_2(x) = 0.$

Inviscid Case: "Negative" Results

The Euler equations: $C_3(x) = 0, \quad \dot{C}_1(x) + 2b\, C_2(x) = 0.$

Trivial (purely rotational) Solution

The purely rotational flow with $F = G \equiv 0,\ \Omega \equiv C_\omega$ is a solution for every $b > 0$.

Inviscid Case: "Negative" Results

The Euler equations: $C_3(x) = 0, \quad \dot{C}_1(x) + 2b\, C_2(x) = 0.$

Trivial (purely rotational) Solution

The purely rotational flow with $F = G \equiv 0,\ \Omega \equiv C_\omega$ is a solution for every $b > 0$.

No Nontrivial Solutions for $b \geq 2$

If $b \geq 2$, then no nontrivial solutions of the form $\mathbf{v} = \dfrac{\mathbf{K}(x)}{r^b}$ exist.

Inviscid Case: "Negative" Results

The Euler equations: $C_3(x) = 0, \quad \dot{C}_1(x) + 2b\, C_2(x) = 0.$

Trivial (purely rotational) Solution

The purely rotational flow with $F = G \equiv 0,\ \Omega \equiv C_\omega$ is a solution for every $b > 0$.

No Nontrivial Solutions for $b \geq 2$

If $b \geq 2$, then no nontrivial solutions of the form $\mathbf{v} = \dfrac{\mathbf{K}(x)}{r^b}$ exist.

Instability for $1 < b < 2$

If $1 < b < 2$, then any nontrivial solution of the form $\mathbf{v} = \dfrac{\mathbf{K}(x)}{r^b}$ is unstable.

Inviscid Case: "Positive" Results

Nontrivial Solutions for $b = 1$

If $b = 1$, then every solution of the form $\mathbf{v} = \dfrac{\mathbf{K}(x)}{r^b}$ satisfies, for $c \in \mathbb{R}$,

$$\Omega \equiv C_\omega, \qquad F = c\sqrt{x(1-x)}, \qquad G = c\,\frac{(1-2x)\sqrt{1+x}}{2\sqrt{x}}.$$

Inviscid Case: "Positive" Results

Nontrivial Solutions for $b = 1$

If $b = 1$, then every solution of the form $\mathbf{v} = \dfrac{\mathbf{K}(x)}{r^b}$ satisfies, for $c \in \mathbb{R}$,

$$\Omega \equiv C_\omega, \qquad F = c\sqrt{x(1-x)}, \qquad G = c\,\frac{(1-2x)\sqrt{1+x}}{2\sqrt{x}}.$$

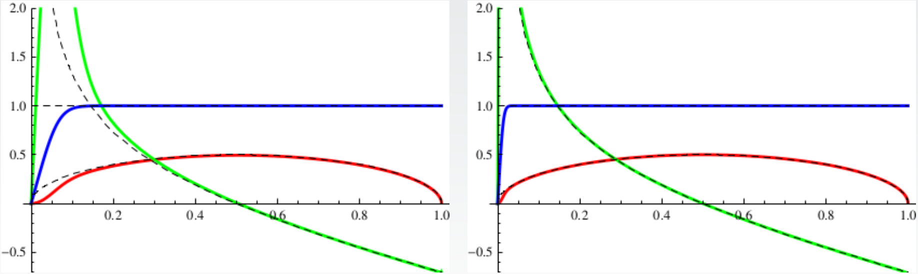

Inviscid Case: “Positive” Results

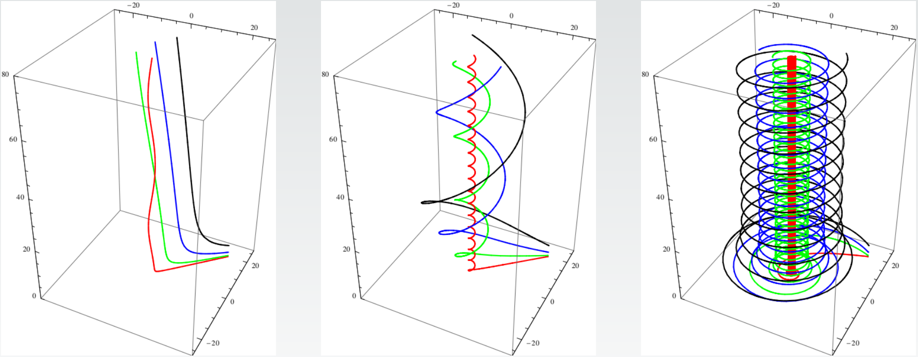

Inviscid Case: "Positive" Results

Nontrivial Numerical Solutions for $0 < b < 1$

For $0 < b < 1$, numerical simulations indicate the existence of solutions that are stable with respect to axisymmetric perturbations.

Inviscid Case: “Positive” Results

Nontrivial Numerical Solutions for $0 < b < 1$

For $0 < b < 1$, numerical simulations indicate the existence of solutions that are stable with respect to axisymmetric perturbations.

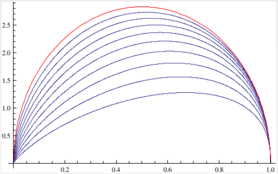

F

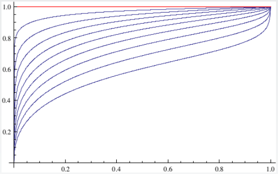

Ω

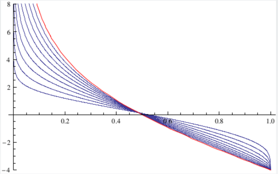

G

Outline

Summary

- For **viscous case**: No axisymmetric solutions with $b \neq 1$

Summary

- For **viscous case**: No axisymmetric solutions with $b \neq 1$
- For **inviscid case**: No axisymmetric solutions for $b \geq 2$

Summary

- For **viscous case**: No axisymmetric solutions with $b \neq 1$
- For **inviscid case**: No axisymmetric solutions for $b \geq 2$
- For **inviscid case**: Instability of axisymmetric solutions for $1 < b < 2$

Summary

- For **viscous case**: No axisymmetric solutions with $b \neq 1$
- For **inviscid case**: No axisymmetric solutions for $b \geq 2$
- For **inviscid case**: Instability of axisymmetric solutions for $1 < b < 2$
- For **inviscid case**: Numerical solutions for $0 < b < 1$ are consistent with Serrin's work, and are stable in the range of fractional powers consistent with mobile radar studies

AUGSBURG COLLEGE UNIVERSITY of ST. THOMAS

Summary

- For **viscous case**: No axisymmetric solutions with $b \neq 1$
- For **inviscid case**: No axisymmetric solutions for $b \geq 2$
- For **inviscid case**: Instability of axisymmetric solutions for $1 < b < 2$
- For **inviscid case**: Numerical solutions for $0 < b < 1$ are consistent with Serrin's work, and are stable in the range of fractional powers consistent with mobile radar studies
- **Thank you!**

Cai's Results

2540 MONTHLY WEATHER REVIEW VOLUME 133

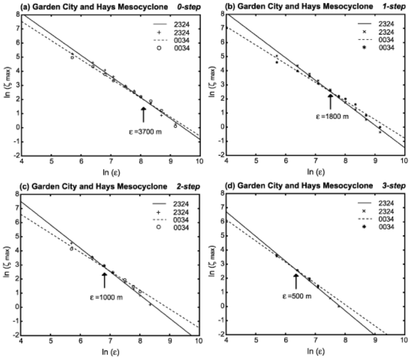

FIG. 4. Comparisons between the vorticity lines of the Garden City and Hays mesocyclones obtained through a (a) zero-step, (b) one-step, (c) two-step, and (d) three-step Leise filter on dual-Doppler winds. Solid black and dashed black lines represent the Garden City mesocyclone at 2324 UTC and the Hays mesocyclone at 0034 UTC, respectively.

Wurman's Results

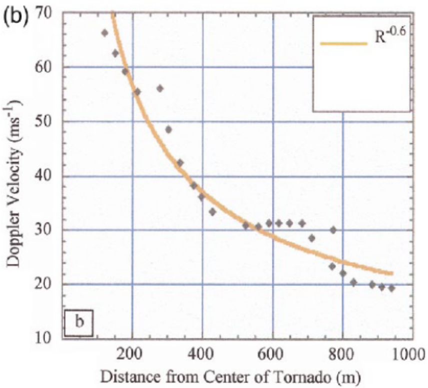

FIG. 21. Distribution of Doppler velocities vs distance from center of tornado. (b) Winds on either side of tornado did not appear to exhibit R^{-1} dependence as predicted by conservation of angular momentum during inflow. Winds in the core region might have been underestimated due to observation aspect ratio limitations, but the general trend in this profile and most others was $V \sim R^{-0.6}$. Best exponential fit for innermost 1000 m of tornado for this profile is shown in (b).